

## Generalized Operations on Maps\*

Mircea V. Diudea,<sup>a,\*\*</sup> Monica Stefu,<sup>a</sup> Peter E. John,<sup>b,\*\*</sup> and Ante Graovac<sup>c,d</sup>

<sup>a</sup>Faculty of Chemistry and Chemical Engineering, Babeş-Bolyai University, 3400 Cluj, Romania

<sup>b</sup>Technical University Ilmenau, Institute of Mathematics, PSF 100565, D-98684 Ilmenau, Germany

<sup>c</sup>The Ruđer Bošković Institute, P.O. Box 180, HR-10002 Zagreb, Croatia

<sup>d</sup>Faculty of Natural Sciences, Mathematics and Education, University of Split, Nikole Tesle 12, HR-21000 Split, Croatia

RECEIVED FEBRUARY 8, 2005; REVISED NOVEMBER 3, 2005; ACCEPTED FEBRUARY 9, 2006

*Keywords* operations on maps  
fullerenes  
perfect Clar structures  
perfect Corannulenic structures  
negatively curved units

A map  $M$  is a combinatorial representation of a closed surface. Convex polyhedra, starting from the Platonic solids and going to spherical fullerenes, can be operated to obtain new objects, with a larger number of vertices and various tiling. Three composite map operations: leapfrog, chamfering and capra, play a central role in the fullerenes construction and their electronic properties. Generalization of the above operations leads to a series of transformations, characterized by distinct, successive pairs in the Goldberg multiplication formula  $m(a,b)$ . Parents and products of most representative operations are illustrated.

### INTRODUCTION

A map  $M$  is a combinatorial representation of a (closed) surface.<sup>1,2</sup> Let us denote the number of vertices, edges, faces by:  $v$ ,  $e$ ,  $f$ , respectively; the vertex degree by  $d$ ; and the face size by  $s$ , in the map. Subscript  $\gg 0 \ll$  will mark the corresponding parameters in the parent map.

Some basic relations in a map were discovered by Euler in the early eighteenth century:<sup>3,4</sup>

$$\sum d v_d = 2e \quad (1)$$

$$\sum s f_s = 2e \quad (2)$$

where  $v_d$  and  $f_s$  are the number of vertices of degree  $d$  and the number of  $s$ -gonal faces, respectively, and  $(d, s \geq 3)$ . The two relations are joined in the famous formula:

$$v - e + f = \chi(M) = 2(1 - g) \quad (3)$$

with  $\chi$  being the Euler characteristic and  $g$  the genus<sup>5</sup> of a graph (*i.e.*, the number of handles attached to the sphere to make it homeomorphic to the surface on which the given graph is embedded;  $g = 0$  for a planar graph and 1 for a toroidal graph). Positive/negative  $\chi$  values indicate positive/negative curvature of a lattice. This formula is useful for checking the consistence of an assumed structure.

Nuclearity of fullerene polyhedra can be counted by Goldberg's<sup>6</sup> relation:

$$m = (a^2 + ab + b^2); \quad a \geq b \quad a + b > 0 \quad (4)$$

which predicts the multiplication factor  $m$  in a 3-valent map transformed by a given operation (see below). The

\* Dedicated to Edward C. Kirby on the occasion of his 70<sup>th</sup> birthday.

\*\* Authors to whom correspondence should be addressed.

(M.V.D., E-mail: diudea@chem.ubbcluj.ro; P.E.J., E-mail: peter.john@mathematic.TU-Ilmenau.de)

$m$  factor is related to the formula giving the volume of a truncated pyramid, of height  $h$ :  $V = mh/3$ , from the ancient Egypt.

This paper is organized as follows: the next (second) section presents some classical composite operations, with definitions given in terms of simple map operations; the third section deals with generalized operations, inspired by Goldberg's representation of polyhedra in the  $(a,b)$  »inclined coordinates«; the fourth section presents some molecular realizations of these composite operations, both as closed and open objects. The last two sections provide a summary of the paper and the references, respectively.

## CLASSICAL COMPOSITE OPERATIONS

We are restricted here to the most important composite operations, assuming that the basic, simple operations, such as: Dual, Medial, Stellation, Truncation, Snub, *etc.*, are known. The reader can consult some previously published papers.<sup>1,2,7</sup>

LEAPFROG Le (tripling) operation<sup>8-12</sup> can be written as:

$$\text{Le}(M) = \text{Du}(P_3(M)) = \text{Tr}(\text{Du}(M)) \quad (5)$$

where  $P_3$  is a particular case of the Polygonal  $P_s$  capping ( $s = 3, 4, 5$ ), realizable<sup>13,14</sup> by (i) adding a new vertex in the center of the face, (ii) putting  $s-3$  points on the boundary edges, and (iii) connecting the central point with one vertex (end points included) on each edge. In this way, the parent face is covered by trigons ( $s = 3$ ), tetragons ( $s = 4$ ) and pentagons ( $s = 5$ ). The  $P_3$  operation is also called stellation or (centered) triangulation.

A sequence of stellation-dualization rotates the parent  $s$ -gonal faces by  $\pi/s$ . Leapfrog operation is illustrated, for a pentagonal face, in Figure 1.

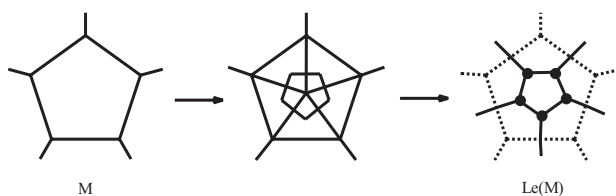


Figure 1. Leapfrogging a pentagonal face of a trivalent map.

A bounding polygon, of size  $2d_0$ , is formed around each original vertex. In the most frequent cases of 4- and 3-valent maps, the bounding polygon is an octagon and a hexagon, respectively.

The following formulas account for lattice parameters of the transformed map:

$$\text{Le}(M): \quad v = s_0 f_0 = d_0 v_0; \quad e = 3e_0; \quad f = v_0 + f_0; \\ m(1,1) = 3 \quad (6)$$

In trivalent maps  $d_0 = 3$ , so that  $\text{Le}(M)$  is also called a tripling operation. Note that the vertex degree in  $\text{Le}(M)$  is always 3, as a consequence of dualization of a triangulation.

A nice example of using the Le operation is:  $\text{Le}(\text{Dodecahedron}) = \text{Fullerene } C_{60}$ . The leapfrog operation can be used to isolate the parent faces by surrounding bounding polygons. The transformed Le-fullerenes have a closed shell  $\pi$ -electronic structure.<sup>2</sup>

CHAMFERING (quadrupling) Q is another composite operation, achieved by the sequence:<sup>6,13,14</sup>

$$Q(M) = E_-(\text{Tr}_{P_3}(P_3(M))) \quad (7)$$

where  $E_-$  means the (old) edge deletion in the truncation  $\text{Tr}_{P_3}$  of the new, face centered, vertices introduced by the  $P_3$  capping (Figure 2). The old vertices are preserved.

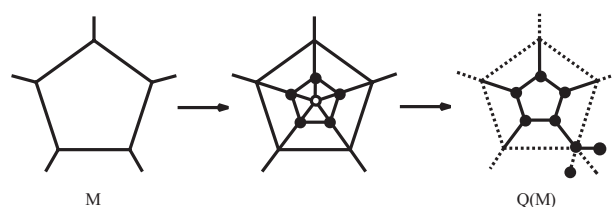


Figure 2. Quadrupling a pentagonal face of a trivalent map.

The following formulas relate lattice parameters of the transformed map to those of the parent map:

$$Q(M): \quad v = (d_0 + 1)v_0; \quad e = 4e_0; \quad f = f_0 + e_0; \\ m(2,0) = 4 \quad (8)$$

Q operation leaves the initial orientation of the polygonal faces unchanged. Note that the chamfering of a 4-valent map is not a regular graph anymore (because of the mixing of the new trivalent vertices with the parent 4-valent ones). Only a 3-valent map is chamfered to a 3-regular graph.

Q always isolates the parent faces by hexagons. An example of this operation is:  $Q(\text{Dodecahedron}) = \text{Fullerene } C_{80}$ . The transformed Q-fullerenes preserve the  $\pi$ -electronic structure of the parents.<sup>14</sup>

The »chamfering« (edge chamfering being equivalent to vertex truncation)<sup>6</sup> is most often called »quadrupling«, by the vertex multiplication  $m = 4$ , in trivalent maps.

CAPRA Ca (septupling) – the goat is the romanian equivalent of the English children's game leapfrog. It is a composite operation,<sup>15</sup> necessarily coming third, by the Goldberg's<sup>6</sup> multiplying factor  $m(2,1)$ .

The transformation can be written as:<sup>14</sup>

$$\text{Ca}(M) = \text{Tr}_{P_5}(P_5(M)) \quad (9)$$

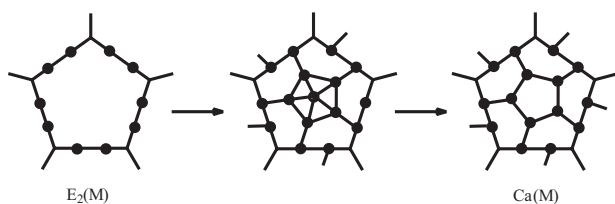


Figure 3. Capping a pentagonal face of a trivalent map.

with  $\text{Tr}_{P_5}$  meaning the truncation of new, face centered, vertices introduced by the  $P_5$  capping (Figure 3). Note that,  $P_5$  involves an  $E_2$  (*i.e.*, edge trisection) operation.

Ca isolates any face of  $M$  by its own hexagons, which are not shared with any old face (in contrast to Le or Q). The transformed Ca-fullerenes preserve the  $\pi$ -electronic shell type of the parents.<sup>14</sup>

Ca operation can continue with an  $E_n$  homeomorphic transformation of the edges bounding the parent-like faces (*i.e.*, those resulting from  $\text{Tr}_{P_5}$ ), thus resulting in open maps with all polygons of the same  $(6+n)$  size. This last simple operation is hereafter denoted<sup>13,14</sup> by  $\text{Op}_n$ .

The sequence leading to open objects within this operation can be written as:

$$\text{Op}_n(\text{Ca}(\text{M})) = \text{Op}_n(\text{Tr}_{P_5}(\text{P}_5(\text{M}))) \quad (10)$$

When  $n = 1$ , this specification is omitted. The Op objects (*i.e.*, molecules) have an open-shell  $\pi$ -electronic structure, eventually including non-bonding orbitals.

Table I lists the net parameters in Capra transforms,<sup>15</sup> either in simple or iterative application to finite or infinite (*i.e.*, open) objects.

According to the  $m$ -value in trivalent maps, Capra is a septupling  $S_1$  operation. Another septupling operation  $S_2$  was defined in Ref. 13.

TABLE I. Parameters transformed by the iterative Ca operation

Operation	Parameter
$\text{Ca}(\text{M})$	$v_1 = v_0 + 2e_0 + s_0f_0 = (2d_0 + 1)v_0$ $e_1 = 7e_0$ $f_1 = s_0f_0 + f_0$
$\text{Op}(\text{Ca}(\text{M}))$	$v_{1\text{Op}} = v_1 + s_0f_0 = (3d_0 + 1)v_0$ $e_{1\text{Op}} = 9e_0$ $f_{1\text{Op}} = f_1 - f_0 = s_0f_0$
$\text{Ca}_2(\text{M})$	$v_2 = v_1 + 2e_1 + \sum sf_{1,s} = v_1 + 2e_1 + 7s_0f_0 = v_0 + 32e_0$ $e_2 = 7^2 e_0$ $f_2 = \sum sf_{1,s} + f_0 = 8s_0f_0 + f_0$
$\text{Op}(\text{Ca}_2(\text{M}))$	$v_{2\text{Op}} = v_{1\text{Op}} + 2e_{1\text{Op}} + 7f_{1\text{Op}} = v_0 + 38e_0$ $e_{2\text{Op}} = 3v_0 + 108e_0$ $f_{2\text{Op}} = (7+1)f_{1\text{Op}} = 16e_0$
$\text{Ca}_n(\text{M})$	case $d_0 > 3$ $v_n = 8v_{n-1} - 7v_{n-2}$ ; $n \geq 2$

Only a 3-valent regular map leads to a regular 3-valent graph in Capra; clearly, maps/graphs of a degree greater than 3 will not be regular anymore.

Since pentangulation of a face can be done either clockwise or counter-clockwise, it results in an enantiomeric pair of objects:  $\text{CaS}(\text{M})$  and  $\text{CaR}(\text{M})$ , in terms of the sinister/rectus stereochemical isomers.<sup>15</sup> Figure 4 illustrates the Schlegel projections of such a pair derived from the cube.

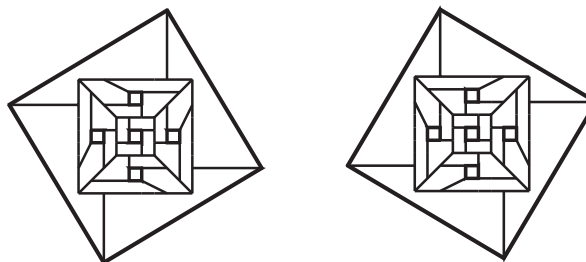
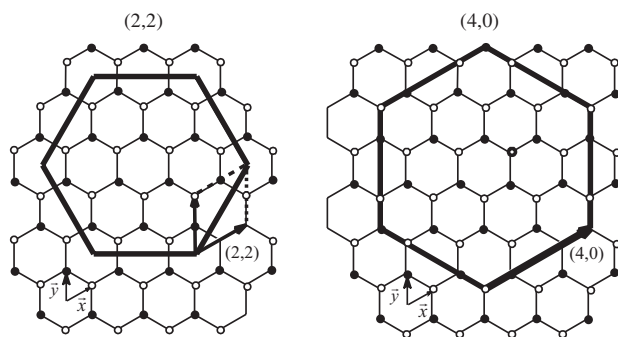
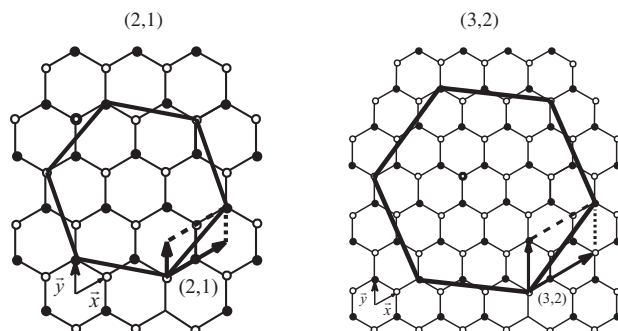


Figure 4. Enantiomeric pair of Capra transforms of the cube (Schlegel projection).

Sequence  $\text{CaS}(\text{CaS}(\text{M}))$  results in a twisted transform, while  $\text{CaR}(\text{CaS}(\text{M}))$  will straighten the (central part of) structure. Sequence  $\text{Du}(\text{Op}(\text{Ca}(\text{M})))$  is just the snub  $\text{Sn}(\text{M})$ , this transform being a chiral one. Examples will be given below.

## GENERALIZED OPERATIONS

One of us (P. E. J.) has proposed a generalization of operations on maps, inspired by the work of Goldberg,<sup>6</sup> and its representation of polyhedra in the  $(a,b)$  »inclined coordinates« ( $60^\circ$  between axes). The nuclearity multiplicity factor  $m$  is given by Eq. (4).

Figure 5. Generalized  $(a, a)$  and  $(a, 0)$  operations.Figure 6. Generalized  $(a, b)$  operation:  $a = b + 1$ .

Figures 5 and 6 illustrate the method on a hexagonal face. The points of the »master« hexagon must lie either in the center of a lattice hexagon or on a lattice vertex. The edge length of the parent hexagon is counted by the primitive lattice vectors.

A similar procedure was used by Coxeter,<sup>16</sup> who built up icosahedral polyhedra/fullerenes as dual master triangular patches, represented by pairs of integers.

Some of the generalized composite operations, corresponding to non-prime  $m$ , can be expressed as operation sequences, as shown in Table II. It is obvious that  $(a, a)$  and  $(a, 0)$  operations provide achiral products (*e.g.*, fullerenes of the full  $I_h$  point group symmetry) while  $(a, b)$ ,  $a \neq b$ , result in chiral transformed maps (*e.g.*, fullerenes of the rotational  $I$  point group symmetry). The  $(a, 0)$  operations produce non-rotated maps. The above generalized operations, as implemented in the software package CageVersatile,<sup>17</sup> work on any face and vertex-degree type maps. The only problem in applying the algorithm appears in cases of odd-fold master faces, centered at a point, as is the case of  $(3, 1)$  operation. In such cases, a different procedure was used.

In the case of trivalent regular maps, relations (1) and (2) can be rewritten as:

$$3 \cdot v_0 = 2 \cdot e_0 = s_0 \cdot f_0 \quad (11)$$

TABLE II. Inclined coordinates  $(a, b)$ , multiplication factor  $m = (a^2 + ab + b^2)$ , number of atoms  $N$  and operation symbols (running on the dodecahedral  $C_{20}$  fullerene)

	$(a, b)$	$m$	$N$	Operation	Obs.
1	(1, 0)	1	20	$I$	Identity
2	(1, 1)	3	60	$Le_{1,1}$	Rotated by $\pi / s$ ; achiral
3	(2, 0)	4	80	$Q_{2,0}$	Non-rotated; achiral
4	(2, 1)	7	140	$Ca_{2,1}$	Rotated by $\pi / 2s$ ; chiral
5	(2, 2)	12	240	$Le_{1,1}, Q_{2,0}$	Rotated by $\pi / s$ ; achiral
6	(3, 0)	9	180	$Le_{1,1}, Le_{1,1}$	Non-rotated; achiral
7	(3, 1)	13	260	–	Rotated; chiral
8	(3, 2)	19	380	–	Rotated; chiral
9	(3, 3)	27	540	$Le_{1,1}, Le_{1,1}, Le_{1,1}$	Rotated by $\pi / s$ ; achiral
10	(4, 0)	16	320	$Q_{2,0}, Q_{2,0}$	Non-rotated; achiral
11	(4, 1)	21	420	$Le_{1,1}, Ca_{2,1}$	Rotated; chiral <sup>(a)</sup>
12	(4, 2)	28	560	$Q_{2,0}, Ca_{2,1}$	Rotated by $\pi / 2s$ ; chiral
13	(4, 3)	37	740	–	Rotated; chiral
14	(4, 4)	48	960	$Le_{1,1}, Q_{2,0}, Q_{2,0}$	Rotated by $\pi / s$ ; achiral
15	(5, 0)	25	500	–	Non-rotated; achiral
16	(5, 1)	31	620	–	Rotated; chiral
17	(5, 2)	39	780	–	Rotated; chiral
18	(5, 3)	49	980	$Ca_{2,1}, Ca_{2,1}$	chiral / achiral <sup>(a)</sup>
19	(5, 4)	61	1220	–	Rotated; chiral
20	(5, 5)	75	1500	–	Rotated; achiral

<sup>(a)</sup> Achiral, when the sequence  $CaR(CaS(M))$  is used.

Keeping in mind the multiplication factor  $m$  (see Eq. (4)), the number of vertices in the transformed map is:

$$v_1 = m \cdot v_0 \quad (12)$$

Eq. (11) leads to:

$$3 \cdot v_1 = 3 \cdot m \cdot v_0 = 2 \cdot e_1 \quad (13)$$

$$e_1 = \frac{3}{2} \cdot m \cdot v_0 = \frac{3}{2} \cdot m \cdot \frac{2}{3} e_0 = m \cdot e_0 \quad (14)$$

The above operations introduce new hexagons, keeping the original faces. Thus, the number of faces of any size  $s$  in  $M_1$  is:

$$f_{1,s} = f_{1,6} + f_0 \quad (15)$$

Relation (11) becomes:

$$2 \cdot e_1 = \sum s \cdot f_{1,s} = 6 \cdot f_{1,6} + s_0 \cdot f_0 \quad (16)$$

Substitution of  $e_1$  in (16) leads to:

$$f_{1,6} = \frac{m-1}{6} \cdot s_0 \cdot f_0 \quad (17)$$

$$f_{1,s} = \frac{m-1}{6} \cdot s_0 \cdot f_0 + f_0 \quad (18)$$

For the  $n^{\text{th}}$  iterative operation, one deduces:

$$v_n = m^n \cdot v_0 \quad (19)$$

$$e_n = m^n \cdot e_0 \quad (20)$$

$$f_{n,s} = \frac{m^n - 1}{6} \cdot s_0 \cdot f_0 + f_0 \quad (21)$$

Relations (19) to (21) hold for all the presented operations running on a trivalent regular  $M_0$ . In other words, the above relations are true of the 3-valent Platonic solids: tetrahedron T, cube C and dodecahedron D.

For other degree maps, in cases of Le, Q and Ca operations, some relations are presented elsewhere.<sup>18</sup>

## MOLECULAR REALIZATION

This section illustrates the »molecular« realization or, in other words, the transformation of molecules (such as graphitoids) by mathematical operations.

### Closed Objects

It has been established that Le operating on fullerenes provides properly closed  $\pi$ -shell, Clar fullerenes. The Q and Ca operations, more related to each other, generally do not change the shell-type of the parent.

Recall that, according to the Clar theory, any polyhedral map may be searched for a perfect Clar PC structure<sup>2,19</sup> (Figure 7), which is a disjoint set of faces (built up on all vertices in M) whose boundaries form a 2-factor. A  $k$ -factor is a regular  $k$ -valent spanning subgraph. A PC structure is associated with a Fries structure,<sup>20</sup> which is a Kekulé structure having the maximum possible  $v/3$  number of benzenoid (alternating single-double edge) faces. A Kekulé structure is a set of pairwise disjoint edges/bonds of the molecule (over all of its atoms) that coincides with a perfect matching and a 1-factor in Graph Theory. A trivalent polyhedral graph, like that of fullerenes, has a PC structure if and only if it has a Fries structure.<sup>2</sup> Such structures represent total resonant sextet, TRS, benzenoid molecules and are expected to be extremely stable, in the valence bond theory.<sup>2,21</sup> Leapfrog Le is the only operation that provides PC transforms.

Coverings larger than benzene, like naphthalene or azulene (*i.e.*, a pair of pentagonal-heptagonal carbon rings), appear only slightly less favorable in the valence-bond based conjugated circuit theory.<sup>21-24</sup>

By extension, Diudea<sup>13</sup> proposed a corannulenic system (Figure 7b). A Disjoint Corannulenic DCor structure is a disjoint set of corannulenes, all interconnected by essentially single bonds. This represents the connected equivalent of the Fries structure.

Among the above three classical composite operations, Le, Q and Ca, none is able to provide a DCor structure. This is, however, possible by the operation sequence Le(Q(M)) or Q(Le(M)), as shown in Figure 7b. This sequence is equivalent to the generalized (2,2) operation.

Any DCor cage shows also a PC structure, the reciprocal being not necessarily true. The supra-organized corannulenic units are expected to contribute to the stability of the whole molecule. The need for a disjoint Cor system comes from the sense of the (large) ring current. Theoretical calculations by the ipsocentric CTOCD (*i.e.*, continuous transformation of the origin of current density) method<sup>25</sup> show diatropic current circulation, close to the corannulenic external boundary, whose intensity could diminish due to counter-sense currents, in eventual adjacent (*i.e.*, edge sharing) Cor units.<sup>26-28</sup>

Any DCor cage shows also a PC structure, the reciprocal being not necessarily true. The supra-organized corannulenic units are expected to contribute to the stability of the whole molecule. The need for a disjoint Cor system comes from the sense of the (large) ring current. Theoretical calculations by the ipsocentric CTOCD (*i.e.*, continuous transformation of the origin of current density) method<sup>25</sup> show diatropic current circulation, close to the corannulenic external boundary, whose intensity could diminish due to counter-sense currents, in eventual adjacent (*i.e.*, edge sharing) Cor units.<sup>26-28</sup>

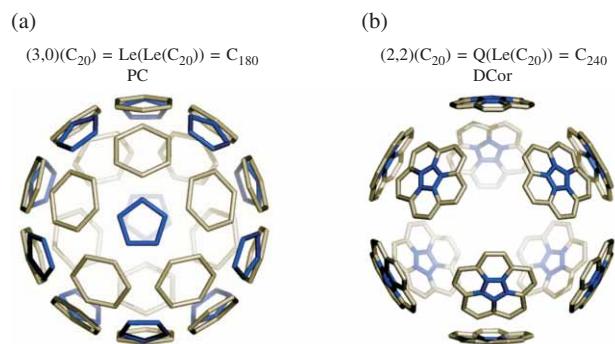


Figure 7. Transforms of  $C_{20}$ , by generalized operations, leading to perfect Clar PC (a) and disjoint corannulenic DCor (b) structures.

The sequence Ca(Le(M)) provides another kind of corannulenic pattern: joint corannulenic JCor, with jointed Cor faces. Looking at the Cor-flowers as »supra« faces, the transform by Ca of a 3-valent Platonic tessellation ( $s$ , 3) remains a Platonic covering, but now it must be written as  $([s]Cor, 3)$ ,  $s$  being the size of the core polygon.

As shown above, if a molecule shows a DCor structure, additional stabilization is expected. It is also possible for such molecules to behave in the magnetic field similarly to planar corannulenes, as investigated by several authors.<sup>26–28</sup> We hope that the hypothesis concerning DCor (see also Refs. 29–32) will be proved in the near future.

As mentioned above, operations  $(a, b)$ ,  $a \neq b$  provide chiral transformed maps. It is, however, possible for the horizontal edge of the parent hexagon to be inclined either to the right or to the left, thus resulting in pair operations and enantiomeric products (see Figure 4).

If a composite operation includes an even repetition of a pro-chiral operation, the sequence of one kind pro-chiral operation will lead to either a chiral transform or an achiral object, the last one in the case of 1:1 ratio of pro-enantiomeric operations (see Figure 8).

$(5,3)(C) = CaS(CaS(C)); m = 49; v = 392$  (Rotated; chiral)       $(7,0)(C) = CaR(CaS(C)); m = 49; v = 392$  (Non-rotated; achiral)

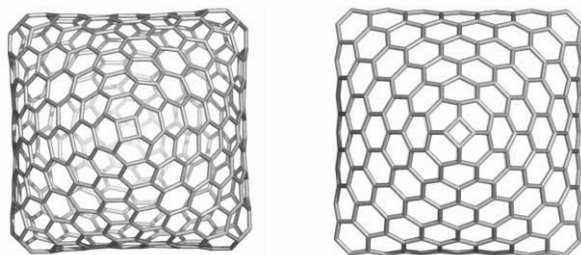


Figure 8. A pair of Capra transforms of the cube.

### Open structures

A sequence of different operations enables to construct various objects, with either positive or negative curvature.<sup>15, 33–36</sup>

Recall that an orientable surface  $S$  (*i.e.*, having two sides) is characterized by the Euler parameter  $\chi(M) = 2(1 - g)$  (see also Eq. (3)).  $\chi(M)$  is directly calculable by the genus<sup>5</sup>  $g$ , being the number of holes made in a plastic sphere to make it homeomorphic to  $S$ . Positive/negative  $\chi$  values indicate positive/negative curvature of a lattice embedded in  $S$ . Embedding is a representation of a graph on a closed surface such that no crossing lines appear.<sup>5,37</sup>

Negative curvature can be induced in graphite (the reference, of zero curvature) by replacing hexagons by sevenfold, or larger sized rings. Such nets cannot form closed polyhedra, in contrast to the objects derived from graphite by introducing pentagons or smaller rings, which

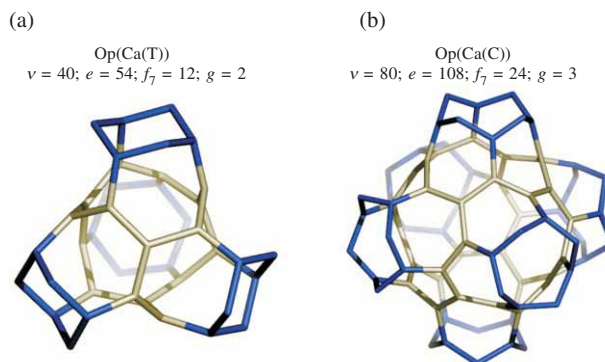


Figure 9. Opening Op operation leads to negative curvature lattices, embedded as repeat units in genus 2 and 3 surfaces.

bring positive curvature, causing cage closure. Thus, negatively curved structures belong to infinite periodic surfaces, with zero mean curvature.

The operation leading to open (repeat) units is  $Op_n$ , which is an  $E_n$  homeomorphic transformation of the parent faces. Most often  $n = 1$ , thus being omitted. It can be associated with any composite operation. In this respect, the (2,1) Capra operation is particularly suitable.<sup>15</sup> Figure 9 illustrates the  $Op(Ca(M))$  sequence.

Open (transformed) maps can no longer be embedded in a surface of genus zero (*e.g.*, in the plane or the sphere). Thus, according to (3), negative  $\chi$  values need  $g > 1$  (see Figure 9).

The genus<sup>5</sup> of an open Capra object,  $Op(Ca(M))$ , is calculable by using the results from Table I and Eq. (3), as:<sup>15</sup>

$$\chi(Op(Ca(M))) = v_{1Op} - e_{1Op} + f_{1Op} = v_0 - e_0 = 2 - 2g \quad (22)$$

$$g = (2 - v_0 + e_0) / 2 = f_0 / 2 \quad (23)$$

Relation (23) arises from the spherical character of the parent polyhedron, for which the Euler relation is written as:  $v_0 - e_0 + f_0 = 2$ . Since  $f_0$  is just the number of open faces, (23) can be extended to any open object, derived by a composite operation from a spherical polyhedron.

Clearly, lattices with  $g > 1$  will have negative  $\chi(Op(M))$  and consequently negative curvature. For the five platonic solids, the genus of the corresponding  $(Op(Ca(M)))$  is: 2 (Tetrahedron); 3 (Cube); 4 (Octahedron); 6 (Dodecahedron), and 10 (Icosahedron).

Note that  $Op(Ca(M))$  leads to the Platonic (7,3) covering of negatively curved units. An interesting example of using the above operation sequence is as follows: the Ca transform of Dodecahedron (Figure 10a) is opened by  $Op_1$  (Figure 10b) and then capped by appropriate all pentagon decorated caps. This is just the way<sup>13</sup> to hypothetical fullerenes,<sup>38</sup> eventually covered only by pentagons and heptagons.

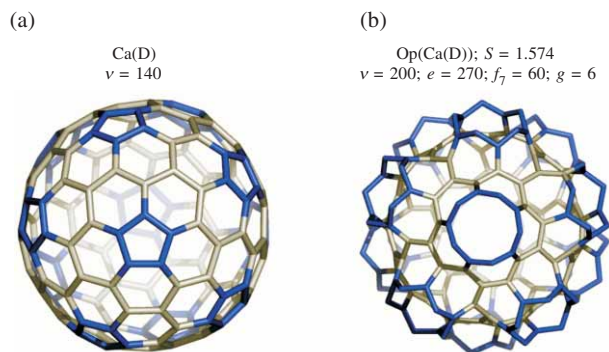


Figure 10. Closed and open objects by Capra.

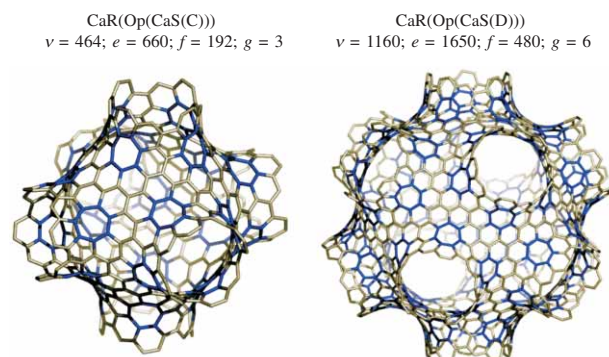


Figure 11. Units of negative curvature, derived by operation sequences from the cube and dodecahedron.

Subsequent transformation of open objects leads to more relaxed units (Figure 11). Such open, negatively curved units can be viewed as rational models for 3D junctions of nanotubes.<sup>33,39</sup>

Using the building block  $\text{Op(Ca(T))}$ , Diudea<sup>13</sup> constructed a supra-molecular (open) dodecahedron, a multi-torus of genus 21, entirely covered by heptagons  $F_7$  (Figure 12a). A new capping leads to a more relaxed object (Figure 12b). Such supra-dodecahedra represent one of the twin labyrinths interlaced in construction of the FRD-type surface; they could appear in a self-assembling process in the synthesis of nanoporous schwarzites.<sup>40–42</sup>

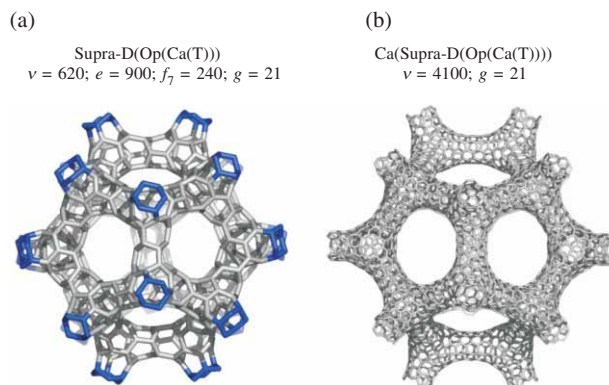


Figure 12. Supramolecular structures built-up by tetrahedral units.

The sequence  $\text{Le(Op(Ca(M)))}$  enables a covering by disjoint azulenic (5,7) units,<sup>13</sup> shown as infinite repeat units in Figure 13. The building block  $\text{Le(Op(Ca(T)))}$  can be used<sup>13</sup> to construct the supra-dodecahedron in Figure 13b, entirely covered by azulenic disjoint units. They represent fully-resonant-azulenoid objects (of  $g > 0$ ), in terms of Kirby's extension<sup>23,43</sup> of the Clar theory<sup>19</sup> on benzenoid systems.

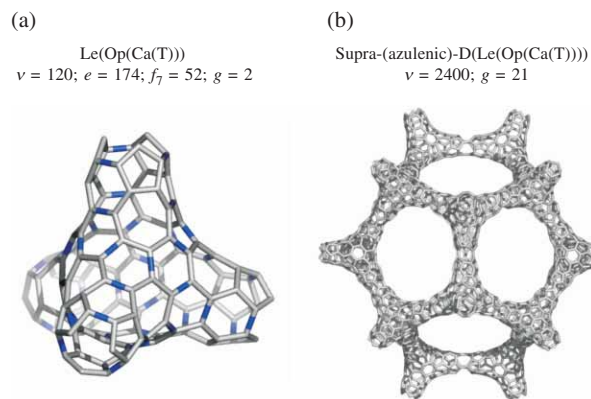


Figure 13. Units covered by disjoint azulenic pairs, representing fully-resonant-azulenoid (aromatic) structures.

## CONCLUSIONS

Convex polyhedra, starting from the Platonic solids and going to spherical fullerenes, can be generated by map operations.

Three composite map operations: leapfrog, chamfering and capra, have been analyzed with respect to their characteristics.

Generalization of the above operations provided a series of transformations, characterized by distinct, successive pairs in the Goldberg multiplication formula  $m(a,b)$ .

Parents and products of most representative operations have been illustrated, both as finite cages or infinite repeat units.

## REFERENCES

1. T. Pisanski and M. Randić, in: C. A. Gorini, (Ed.), *Geometry at Work, Math. Assoc. Am.* **53** (2000) 174–194.
2. P. W. Fowler and T. Pisanski, *J. Chem. Soc., Faraday Trans.* **90** (1994) 2865–2871.
3. L. Euler, *Comment. Acad. Sci. I. Petropolitanae* **8** (1736) 128–140.
4. L. Euler, *Novi Comment. Acad. Sci. I. Petropolitanae* **4** (1758) 109–160.
5. F. Harary, *Graph Theory*, Addison-Wesley, Reading, MA, 1969.
6. M. Goldberg, *Tohoku Math. J.* **43** (1937) 104–108.

7. M. V. Diudea, P. E. John, A. Graovac, M. Primorac, and T. Pisanski, *Croat. Chem. Acta* **76** (2003) 153–159.
8. P. W. Fowler, *Phys. Lett.* **131** (1986) 444–450.
9. P. W. Fowler and J. I. Steer, *J. Chem. Soc., Chem. Commun.* (1987) 1403–1405.
10. P. W. Fowler and K. M. Rogers, *J. Chem. Soc., Faraday Trans.* **94** (1998) 1019–1027.
11. P. W. Fowler and K. M. Rogers, *J. Chem. Soc., Faraday Trans.* **94** (1998) 2509–2514.
12. M. V. Diudea and P. E. John, *MATCH, Commun. Math. Comput. Chem.* **44** (2001) 103–116.
13. M. V. Diudea, *Forma* **19** (2004) 131–136.
14. M. V. Diudea, in: M. V. Diudea (Ed.), *Nanostructures-Novel Architecture*, NOVA, New York, 2005, pp. 203–242.
15. M. V. Diudea, *Studia Univ. Babeş-Bolyai (Cluj)* **48** (2003) 3–16.
16. H. S. M. Coxeter, *Regular polytopes*, 3rd ed., Dover Pubs, Dover, 1973.
17. M. Stefu and M. V. Diudea, *CageVersatile 1.3*, Babeş-Bolyai University (Cluj), 2003.
18. M. Stefu, M. V. Diudea, and P. E. John, *Studia Univ. Babeş-Bolyai (Cluj)* **50** (2005) 165–175.
19. E. Clar, *The Aromatic Sextet*, Wiley, New York, 1972.
20. K. Fries, *J. Liebigs Ann. Chem.* **454** (1927) 121–324.
21. J. R. Dias, *J. Chem. Inf. Comput. Sci.* **39** (1999) 144–150.
22. D. J. Klein and H. Zhu, in: A. T. Balaban, (Ed.), *From Chemical Topology to Three-Dimensional Geometry*, Plenum Press, New York, 1997, pp. 297–341.
23. E. C. Kirby, *MATCH, Commun. Math. Comput. Chem.* **33** (1996) 147–156.
24. J. V. Knop, W. R. Muller, K. Szymanski, S. Nikolić, and N. Trinajstić, *MATCH, Commun. Math. Comput. Chem.* **29** (1993) 81–106.
25. T. A. Keith and R. F. W. Bader, *Chem. Phys. Lett.* **210** (1993) 223–231.
26. A. Acocella, R. W. A. Havenith, E. Steiner, P. W. Fowler, and L. W. Jenneskens, *Chem. Phys. Lett.* **363** (2002) 64–72.
27. P. W. Fowler and E. Steiner, *Chem. Phys. Lett.* **363** (2002) 259–266.
28. P. Lazzeretti, in: J. W. Emsley, J. Feeney, and L. H. Sutcliffe (Eds.), *Progress in Nuclear Magnetic Resonance Spectroscopy*, Elsevier, Amsterdam **36** (2000) 1–88.
29. H. Hosoya, Y. Tsukano, K. Nakada, S. Iwata, and U. Nagashima, *Croat. Chem. Acta* **77** (2004) 89–95.
30. H. Hosoya, Y. Tsukano, M. Ohuchi, and K. Nakada, in: M. Doyama, J. Kihara, M. Tanaka, and R. Yamamoto (Eds.), *Computer Aided Innovation of New Materials II*, Elsevier, 1993, pp. 155–158.
31. J.-I. Aihara, T. Yamabe, and H. Hosoya, *Synth. Met.* **64** (1994) 309–313.
32. D. J. Klein, T. Živković, and A. T. Balaban, *MATCH, Commun. Math. Comput. Chem.* **29** (1993) 107–130.
33. Cs. L. Nagy and M. V. Diudea, *Studia Univ. Babeş-Bolyai* **48** (2) (2003) 37–46.
34. A. L. Mackay and H. Terrones, *Nature* **352** (1991) 762–762.
35. D. Vanderbilt and J. Tersoff, *Phys. Rev. Lett.* **68** (1992) 511–513.
36. T. Lenosky, X. Gonze, M. Teter, and V. Elser, *Nature* **355** (1992) 333–335.
37. J. L. Gross and T. W. Tucker, *Topological graph theory*, Dover Pubs, Dover, 2001.
38. A. Dress and G. Brinkmann, *MATCH, Commun. Math. Comput. Chem.* **33** (1996) 87–100.
39. Cs. L. Nagy and M. V. Diudea, in: M. V. Diudea (Ed.), *Nanostructures-Novel Architecture*, NOVA, New York, 2005, pp. 311–334.
40. H. A. Schwarz, *Monatsber. Dtsch. Wiss. Acad. Berlin*, 1865.
41. H. A. Schwarz, *Gesammelte Mathematische Abhandlungen*, Springer, Berlin, 1890.
42. G. Benedek, H. Vahedi-Tafreshi, E. Barborini, P. Piseri, P. Milani, C. Ducati, and J. Robertson, *Diamond Relat. Mater.* **12** (2003) 768–773.
43. E. C. Kirby, in: M. V. Diudea (Ed.), *Nanostructures-Novel Architecture*, NOVA, New York, 2005, pp. 175–191.

---

## SAŽETAK

### Poopćene operacije na kartama

**Mircea V. Diudea, Monica Stefu, Peter E. John i Ante Graovac**

Karta je kombinatorni prikaz zatvorene površine. Nad konveksnim poliedrima, od Platonovih tijela pa do kuglastih fullerena, mogu se provoditi razne operacije kako bi se dobili novi objekti s velikim brojem vrhova i raznim prekrivanjima. Tri operacije na kartama, *leapfrog*, *chamfering* i *capra*, igraju središnju ulogu u konstrukciji fullerena i proučavanju njihovih elektronskih svojstava. Poopćenja ovih operacija vode do niza transformacija karakteriziranih uzastopnim i različitim parovima brojeva u Goldbergovoj formuli. Za najvažnije operacije prikazani su roditelji i potomci.